

Logic and Commonsense-Guided Temporal Knowledge Graph Completion

Guanglin Niu¹, Bo Li^{1,2*}

¹ Institute of Artificial Intelligence, Beihang University, Beijing, China

² Hangzhou Innovation Institute, Beihang University, Hangzhou, China

{beihangngl, boli}@buaa.edu.cn

Abstract

A temporal knowledge graph (TKG) stores the events derived from the data involving time. Predicting events is extremely challenging due to the time-sensitive property of events. Besides, the previous TKG completion (TKGC) approaches cannot represent both the timeliness and the causality properties of events, simultaneously. To address these challenges, we propose a Logic and Commonsense-Guided Embedding model (LCGE) to jointly learn the time-sensitive representation involving timeliness and causality of events, together with the time-independent representation of events from the perspective of commonsense. Specifically, we design a temporal rule learning algorithm to construct a rule-guided predicate embedding regularization strategy for learning the causality among events. Furthermore, we could accurately evaluate the plausibility of events via auxiliary commonsense knowledge. The experimental results of TKGC task illustrate the significant performance improvements of our model compared with the existing approaches. More interestingly, our model is able to provide the explainability of the predicted results in the view of causal inference. The source code and datasets of this paper are available at <https://github.com/ngl567/LCGE>.

1 Introduction

Knowledge graph (KG) has been developed rapidly in recent years, which stores facts in the form of (subject, predicate, object). To further exploit the events involving time, temporal KG (TKG) represents each event as a quadruple (subject, predicate, object, time) where the time information can be formulated by a timestamp or time interval. For instance, an event (*Barack Obama*, *Consult*, *Xi Jinping*, 2014-11-11) in a TKG as shown in Figure 1 indicates that this event occurs on the definite date of 2014-11-11.

Temporal KG completion (TKGC) is an essential technique to predict whether some potential events missing in the TKG will occur, i.e., (*Xi Jinping*, *Consult*, *Barack Obama*, 2014-06-15) shown in Figure 1. Particularly, an event is only valid at a specific time namely the timeliness. The existing TKGC approaches can be classified into two categories: (1) the evolution-based models are capable of representing the causality among events to reason

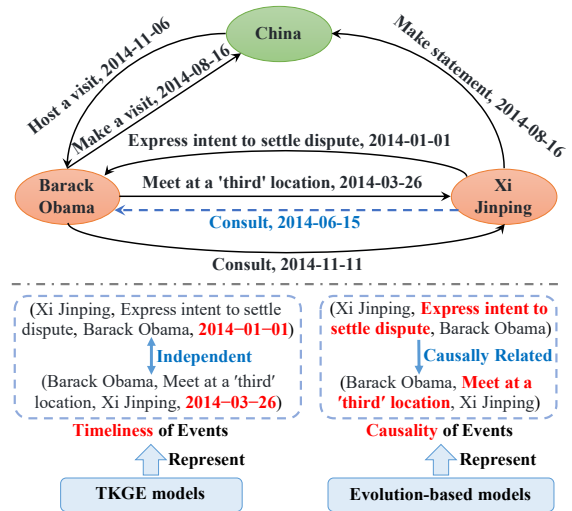


Figure 1: A brief example of the TKG from ICEWS dataset and the TKGC task predicting the missing event (*Xi Jinping*, *Consult*, *Barack Obama*, 2014-06-15). Besides, the existing TKGC models cannot jointly represent the timeliness of events and the causality among events.

the future events, such as Know-Evolve (Trivedi et al. 2017) RE-NET (Jin et al. 2020) and CyGNet (Zhu et al. 2021). As the declaration of causality of events is shown in Figure 1, when two events occur in certain time order, one event has an impact on the other. The event occurring earlier is the reason and the event occurring later is the result. (2) The TKG embedding (TKGE) models, which this paper focuses on, evaluate the plausibility of events via scoring events with embeddings of entities and predicates together with timestamps, including TTransE (Leblay and Chekol 2018), HyTE (Dasgupta, Ray, and Talukdar 2018) and DE-SimplE (Goel et al. 2020). TKGE models regard the events that occur at different times are completely independent and these approaches predict the events at the known time.

However, the previous models face several challenges: (1) the existing TKGC models believe that any TKG simply contains events involving time but they ignore the long-term effective commonsense knowledge implied in the TKG. (2)

* Corresponding author.

The evolution-based models struggle to reason about events with weak correlations to past events while the TKGE models are unable to exploit the causality among events. In summary, all the existing TKGC approaches cannot jointly represent the timeliness and causality of events. (3) Almost all the previous TKGC techniques are data-driven without explainability. Besides, StreamLearner (Omran, Wang, and Wang 2019b) is the only known approach that automatically mines temporal rules from TKGs. However, it merely explores the single pattern that all the atoms in the rule body are restricted at the same time but ignores the diverse temporal rule patterns among events.

To address the above challenges, we develop a novel and effective Logic and Commonsense-Guided Embedding (LCGE) model to represent events more adequately for improving the performance of TKGC. Concretely, we design a temporal rule-guided predicate embedding regularization for learning the causality property of events. Furthermore, a joint event and commonsense-based KG embedding strategy is proposed to score each event via learning the time-sensitive representation involving timeliness and causality as well as the time-independent representation in the view of commonsense. The main contributions of our work include:

- We design a temporal rule-guided regularization strategy to inject the causality among events into predicate embeddings. To the best of our knowledge, it is the first effort to introduce temporal rules into TKGE models.
- We model each event from the perspectives of both the time-sensitive representation and the commonsense, facilitating higher accuracy in predicting missing events.
- The experimental results on three benchmark datasets of TKGs illustrate the significant performance improvements of our model compared with several state-of-the-art baselines. More interestingly, our model could provide explainability via temporal rules.

2 Related Work

2.1 Traditional KGE Models

KGE technique aims to score the plausibility of facts via learning the entity and predicate embeddings. TransE (Bordes et al. 2013) models the interaction among a triple fact via regarding a predicate as the translation operation from subject to object. More advanced approaches represent predicates as rotation operations for modeling the symmetric and anti-symmetric predicates, such as RotatE (Sun et al. 2019), QuatE (Zhang et al. 2019) and DualE (Cao et al. 2021). RESCAL (Nickel, Tresp, and Kriegel 2011) conducts three-order tensor decomposition to calculate the truth values of facts. DistMult (Yang et al. 2015) and ComplEx (Trouillon et al. 2016) simplify RESCAL model with fewer parameters and improve the performance of KG completion.

2.2 Temporal KGE Models

Temporal KGE (TKGE) models extend the traditional KGE approaches by supplementing the time embeddings to represent the time-aware events. TTransE (Leblay and Chekol

2018) adds an extra time embedding in the translation-based score function to represent the timeliness of events. Motivated by the hyper-plane specific to the relation proposed in TransH (Wang et al. 2014), HyTE (Dasgupta, Ray, and Talukdar 2018) projects the entities and predicates into the hyper-plane of a specific time. DE-SimplE (Goel et al. 2020) leverages the diachronic entity embeddings to represent each entity in different timestamps. ATiSE (Xu et al. 2020b) learns the time-aware embeddings of entities and predicates to a Gaussian distribution for representing the time uncertainty. TeRo (Xu et al. 2020a) extends HyTE to learn the time-sensitive entity and predicate embeddings via rotation operation specific to various timestamps (Sun et al. 2019). TComplEx (Lacroix, Obozinski, and Usunier 2020) upgrades ComplEx to score each event via a fourth-order tensor decomposition that introduces time information.

2.3 Rule Learning

According to the symbolic characteristics of KGs, logic rules are naturally suitable for KG completion task. The Horn rule is a typical type of logic rule in the form of $a_1 \Leftarrow a_2 \wedge a_3 \wedge \dots \wedge a_n$, in which a_1 denotes an atom in the rule head (namely head atom) and a_2, \dots, a_n are the atoms in the rule body (namely body atoms). Some effective rule learning algorithms are developed specifically for large-scale KGs relying on rule searching and rule quality evaluation, such as AMIE+ (Galárraga et al. 2015), ScaLeKB (Y.Chen, D.Z.Wang, and S.Goldberg 2016), RuLES (Ho et al. 2018), Anyburl (Meilicke et al. 2019), DRUM (Sadeghian et al. 2019), RLvLR (Omran, Wang, and Wang 2019a) and RNNLogic (Qu et al. 2021). However, these approaches are designed for static KGs rather than TKGs. StreamLearner (Omran, Wang, and Wang 2019b) is the only known algorithm to mine the temporal rules of which all the body atoms are restricted, simultaneously.

3 The Proposed LCGE Model

In this section, we firstly introduce the preliminaries (§3.1). Then, we declare our developed temporal rule learning algorithm with diverse temporal rule patterns (§3.2) and further propose the temporal rule-guided predicate embedding regularization (RGPR) (§3.3). Afterward, the joint event and commonsense-based KGE mechanism (§3.4) together with the overall optimization objective (§3.5) are presented. The whole framework of our model is shown in Figure 2.

3.1 Preliminaries

Temporal Knowledge Graph. The temporal knowledge graph (TKG) is a set of events attached with time information. Each event is represented as a quadruple (s, p, o, t) , in which s and o are subject and object, p denotes the predicate, and t implies the timestamp or time interval. Particularly, an event with a time interval $[t_s, t_e]$ can be converted into two events with timestamps namely (s, p, o, t_s) and (s, p, o, t_e) .

Temporal Rule. A temporal rule is formulated as the conjunction of the atoms attached with time labels. In our work, we focus on the temporal rules in the form of

$$p_{n+1}(x, y, t) \Leftarrow p_1(x, z_1, t_1) \wedge \dots \wedge p_n(z_{n-1}, y, t_n) \quad (1)$$

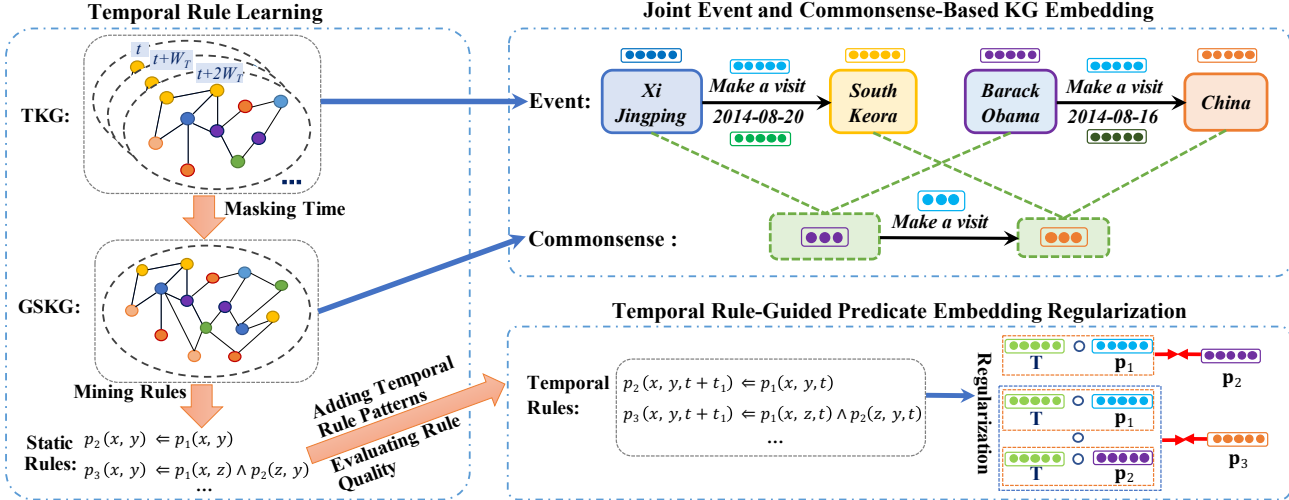


Figure 2: The whole framework of our LCGE model. Commonsense is represented as the interaction between two entity concept embeddings and a predicate embedding. The subject concept embeddings of the two events shown in this figure should be close to each other since they are associated with the same predicate. In the temporal rule-guided predicate embedding regularization module, \mathbf{T} denotes the temporal transformation operator that will be described in section 3.3.

where $p_i (i = 1, \dots, n + 1)$ are the predicates. x, y and $z_j (j = 1, \dots, n - 1)$ denote the entity variables. Particularly, t and $t_l (l = 1, \dots, n)$ indicate the time variables that satisfy the constraint $t_1 \leq t_2 \leq \dots \leq t_n \leq t$. A temporal rule signifies that the rule head will happen if the rule body holds. A grounding of the temporal rule is obtained by replacing the variables with specific entities and timestamps.

3.2 Temporal Rule Learning

We develop a novel static-to-dynamic strategy to mine the temporal rules with various patterns. In the static rule learning stage, we first convert all the quadruple events in training set into triples via masking the time information of each event as shown in Figure 2. Then, we obtain a global static KG (GSKG) consisting of all the triples and mine the static rules from the GSKG by any existing rule learning algorithm such as AMIE+ (Galárraga et al. 2015) or Anyburl (Meilicke et al. 2019). Notably, temporal rules can be regarded as the extension of static rules with various temporal rule patterns.

Formulation of Temporal Rule Patterns. At the dynamic rule learning stage, five temporal rule patterns as shown in Figure 3 are well-designed according to the diverse temporal sequences among atoms as followings:

(1) A length-1 rule in which the two atoms have different timestamps: $p_2(x, y, t + t_1) \Leftarrow p_1(x, y, t)$.

(2) A length-1 rule where the two atoms are valid at the same time: $p_2(x, y, t) \Leftarrow p_1(x, y, t)$.

(3) A length-2 rule that the timestamps of the three atoms are different from each other: $p_3(x, y, t + t_1 + t_2) \Leftarrow p_1(x, z, t) \wedge p_2(z, y, t + t_1)$.

(4) A length-2 rule where the timestamps of the body atoms differ from that of the head atom: $p_3(x, y, t + t_1) \Leftarrow p_1(x, z, t) \wedge p_2(z, y, t)$.

(5) A length-2 rule for the three atoms to be valid at the same time: $p_3(x, y, t) \Leftarrow p_1(x, z, t) \wedge p_2(z, y, t)$.

A detailed description of temporal rule patterns can be found in Appendix A.1.

Quality Evaluation of Temporal Rules. On account of the static rules mined by the existing rule learning algorithms and the proposed five temporal rule patterns, we extend each static rule to be the corresponding candidate temporal rules according to the defined temporal rule patterns.

To evaluate the quality of each candidate temporal rule, we firstly merge the events in the same time window into a sub-graph since some causally related events may occur in the same sub-graph or the adjacent sub-graphs. Then, we search for all the events satisfying the grounding of candidate temporal rules. Specific to a length-1 temporal rule in the general form $p_2(x, y, t + T_1) \Leftarrow p_1(x, y, t)$, it satisfies pattern (1) when $T_1 = 0$ and signifies pattern (2) if $T_1 > 0$. Thereby, following the definition of the evaluation criteria in previous rule learning models (Sadeghian et al. 2019), we propose support degree (SD), standard confidence (SC), and head coverage (HC) of temporal rules as follows:

$$SD = \begin{cases} \#(a, b) : p_1(a, b, t) \wedge p_2(a, b, t), & T_1 = 0 \\ \#(a, b) : \sum_{t_{1i} \in [1, W_T]} p_1(a, b, t) \wedge p_2(a, b, t + t_{1i}), & T_1 > 0 \end{cases} \quad (2)$$

$$SC = \begin{cases} \frac{SD}{\#(a, b) : p_1(a, b, t)}, & T_1 = 0 \\ \frac{1}{|W_T|} \cdot \frac{SD}{\#(a, b) : p_1(a, b, t)}, & T_1 > 0 \end{cases} \quad (3)$$

$$HC = \begin{cases} \frac{SD}{\#(a, b) : p_2(a, b, t)}, & T_1 = 0 \\ \frac{SD}{\#(a, b) : \sum_{t_{1i} \in [1, W_T]} p_2(a, b, t + t_{1i})}, & T_1 > 0 \end{cases} \quad (4)$$

in which W_T denotes the size of the pre-defined time window. The evaluation criteria of length-2 temporal rules are

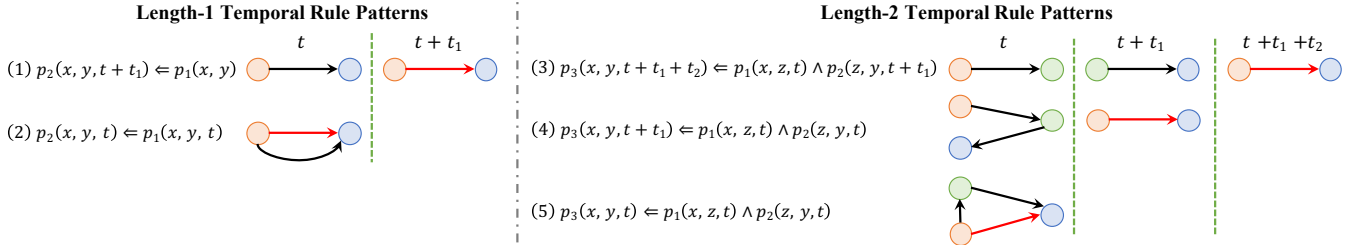


Figure 3: A brief diagram of the proposed five temporal rule patterns. The dots indicate the variables. The red lines denote the predicates in the head atoms while the black lines represent the predicates in the body atoms.

defined similarly to that of length-1 temporal rules and are provided in Appendix A.2.

We acquire the SC and HC of each candidate temporal rule by traversing the timestamp t in accordance with the temporal rules' evaluation criteria. The candidate temporal rules satisfying the thresholds of SC and HC are employed for the following regularization strategy in section 3.3. The entire algorithm of our proposed temporal rule learning module is presented in Appendix A.3.

3.3 The Designed RGPR Mechanism

Based on the generated temporal rules signifying the causality among atoms, we define a time transfer operator \mathbf{T} , which ensures all the atoms in a rule are represented at the same time to calculate their correlations. Take the temporal rule $p_3(x, y, t + t_1 + t_2) \Leftarrow p_1(x, z, t) \wedge p_2(z, y, t + t_1)$ for an instance, projecting the body atom $p_1(x, z, t)$ into the same time window of the head atom requires time transfer operation twice. Furthermore, the temporal rule-guided predicate embedding regularization \mathbf{G} is proposed to inject the causality implied in the temporal rules into predicate embeddings corresponding to each temporal rule pattern:

$$(1) p_2(x, y, t + t_1) \Leftarrow p_1(x, y, t):$$

$$\mathbf{G} = \|(\mathbf{T} \circ \mathbf{p}_{r1}) - \mathbf{p}_{r2}\| \quad (5)$$

$$(2) p_2(x, y, t) \Leftarrow p_1(x, y, t):$$

$$\mathbf{G} = \|\mathbf{p}_{r1} - \mathbf{p}_{r2}\| \quad (6)$$

$$(3) p_3(x, y, t + t_1 + t_2) \Leftarrow p_1(x, e, t) \wedge p_2(e, y, t + t_1):$$

$$\mathbf{G} = \|(\mathbf{T} \circ \mathbf{T} \circ \mathbf{p}_{r1}) \circ (\mathbf{T} \circ \mathbf{p}_{r2}) - \mathbf{p}_{r3}\| \quad (7)$$

$$(4) p_3(x, y, t + t_1) \Leftarrow p_1(x, e, t) \wedge p_2(e, y, t):$$

$$\mathbf{G} = \|(\mathbf{T} \circ \mathbf{p}_{r1}) \circ (\mathbf{T} \circ \mathbf{p}_{r2}) - \mathbf{p}_{r3}\| \quad (8)$$

$$(5) p_3(x, y, t) \Leftarrow p_1(x, e, t) \wedge p_2(e, y, t):$$

$$\mathbf{G} = \|\mathbf{p}_{r1} \circ \mathbf{p}_{r2} - \mathbf{p}_{r3}\| \quad (9)$$

where \mathbf{p}_{r1} , \mathbf{p}_{r2} and \mathbf{p}_{r3} indicate the embeddings of predicates p_1 , p_2 and p_3 , respectively. \circ denotes Hardman product. Particularly, we theoretically prove that the designed \mathbf{G} could model the causality among events in Appendix A.4.

3.4 Joint Event and Commonsense-Based KGE

We take full advantage of the long-term validity of commonsense to evaluate the plausibility of an event accurately since some events that go against commonsense will never happen. Thus, we model each event from the perspective of both time-sensitive and time-independent representations.

To learn the time-sensitive representation of events, inspired by TKGE model TComplEx (Lacroix, Obozinski, and Usunier 2020), we learn the timeliness of each event embodied with the timestamp via four-order tensor decomposition. Besides, the causality among events can be represented via our RGPR mechanism together with the subject and object embeddings. Given an event quadruple (s, p, o, t) , the time-sensitive score function is defined as

$$\begin{aligned} E_1(s, p, o, t) &= \text{Re}(\mathbf{s}^\top \text{diag}(\mathbf{p}_t + \mathbf{p}_r) \bar{\mathbf{o}}) \\ &= \text{Re}\left(\sum_{i=1}^d [\mathbf{s}]_i \cdot [\mathbf{p} \circ \mathbf{t} + \mathbf{p}_r]_i \cdot [\bar{\mathbf{o}}]_i\right) \end{aligned} \quad (10)$$

where $\mathbf{s} \in \mathbb{C}^d$, $\mathbf{p} \in \mathbb{C}^d$, $\mathbf{o} \in \mathbb{C}^d$ indicate the embeddings in the d -dimension complex vector space with regard to s , p and o , respectively. $\bar{\mathbf{o}}$ is the conjugate of \mathbf{o} . Particularly, $\mathbf{p}_t = \mathbf{p} \circ \mathbf{t}$ denotes the predicate embedding constrained by the timestamp t . Meanwhile, \mathbf{p}_r is the causality representation of the predicate p learned by our RGPR mechanism. From Eqs. 5-9, if some events hold, the other events that are causally relevant to these events would have higher scores according to the regularization of predicate embeddings. $[\mathbf{x}]_i$ denotes the i -th value of the complex vector \mathbf{x} . Based on the developed score function in Eq. 10, we could jointly represent the timeliness and the causality of events, facilitating a more sufficient time-sensitive representation of events.

To learn the time-independent representation of commonsense associated with events, the timestamp in each event is masked to convert the event quadruple (s, p, o, t) into the factual triple (s, p, o) . Motivated by some typical commonsense KGs such as ConceptNet (Speer, Chin, and Havasi 2017), commonsense is represented as two concepts linked by a predicate. Therefore, we score each event in the view of commonsense via the learnable concept and predicate embeddings together with the proposed time-independent score function based on commonsense:

$$E_2(s, p, o) = \text{Re}\left(\sum_{i=1}^k [\mathbf{s}_c]_i \cdot [\mathbf{p}_c]_i \cdot [\bar{\mathbf{o}}_c]_i\right) \quad (11)$$

Dataset	#Predicate	#Entity	#Train	#Valid	#Test	Time Span
ICEWS14	230	6,869	72,826	8,941	8,963	2014
ICEWS05-15	251	10,094	368,962	46,275	46,092	2005-2015
Wikidata12k	24	12,554	32,497	4,062	4,062	1479-2018

Table 1: Statistics of the experimental datasets. Time span indicates the range of years in which the events occur.

Temporal Rule Patterns	The Mined Temporal Rules with Confidence
$p_2(x, y, t + t_1) \Leftarrow p_1(x, y, t)$	<i>Host a visit</i> ($x, y, t + t_1$) \Leftarrow <i>Make a visit</i> (x, y, t) 0.45
$p_2(x, y, t) \Leftarrow p_1(x, y, t)$	<i>Mobilize or increase armed forces</i> (x, y, t) \Leftarrow <i>Increase military alert status</i> (x, y, t) 0.33
$p_3(x, y, t + t_1 + t_2) \Leftarrow p_1(x, z, t) \wedge p_2(z, y, t + t_1)$	<i>Express intent to meet or negotiate</i> ($x, y, t + t_1 + t_2$) \Leftarrow <i>Engage in negotiation</i> ⁻¹ (x, z, t) \wedge <i>Express intent to cooperate</i> ($z, y, t + t_1$) 0.27
$p_3(x, y, t + t_1) \Leftarrow p_1(x, y, t) \wedge p_2(x, y, t)$	<i>Protest violently, riot</i> ($x, y, t + t_1$) \Leftarrow <i>Demonstrate or rally</i> (x, y, t) \wedge <i>Make an appeal or request</i> (x, y, t) 0.25
$p_3(x, y, t) \Leftarrow p_1(x, z, t) \wedge p_2(z, y, t)$	<i>Engage in negotiation</i> (x, y, t) \Leftarrow <i>Engage in diplomatic cooperation</i> ⁻¹ (x, z, t) \wedge <i>Express intent to settle dispute</i> (z, y, t) 0.67

Table 2: The cases of temporal rules mined from ICEWS05-15 with respective to each temporal rule pattern.

where $\mathbf{s}_c \in \mathbb{C}^k$, $\mathbf{p}_c \in \mathbb{C}^k$, $\mathbf{o}_c \in \mathbb{C}^k$ represent the concept embeddings in the k -dimension complex vector space with regard to subject s , predicate p and object o , respectively. Particularly, k should be set smaller than d to enhance the abstract feature of entity concept embeddings.

3.5 Optimization Objective

We employ the log-softmax loss function and N3 regularization to design the optimization objective for training:

$$L = \sum_{(s, p, o, t) \in \mathcal{T}} (L_1 + \lambda \cdot L_2) \quad (12)$$

$$L_1 = -\log \left(\frac{\exp(E_1(s, p, o, t))}{\sum_{e_i \in \mathcal{E}} \exp(E_1(e_i, p, o, t))} \right) - \log \left(\frac{\exp(E_1(s, p, o, t))}{\sum_{e_i \in \mathcal{E}} \exp(E_1(s, p, e_i, t))} \right) + \alpha_1 (\|\mathbf{s}\|_3^3 + \|\mathbf{p}_t\|_3^3 + \|\mathbf{p}_r\|_3^3 + \|\mathbf{o}\|_3^3) \quad (13)$$

$$L_2 = -\log \left(\frac{\exp(E_2(s, p, o))}{\sum_{e_i \in \mathcal{E}} \exp(E_2(e_i, p, o))} \right) - \log \left(\frac{\exp(E_2(s, p, o))}{\sum_{e_i \in \mathcal{E}} \exp(E_2(s, p, e_i))} \right) + \alpha_2 (\|\mathbf{s}_c\|_3^3 + \|\mathbf{p}_c\|_3^3 + \|\mathbf{o}_c\|_3^3) \quad (14)$$

in which L_1 and L_2 represent the loss functions specific to the time-sensitive events and time-independent commonsense, respectively. \mathcal{T} and \mathcal{E} are the event set and the entity set in the TKG, respectively. e_i denotes an entity in the entity set \mathcal{E} . α_1 and α_2 are defined as the N3 regularization weights corresponding to entity embeddings and predicate embeddings, respectively. λ is the weight of commonsense representation in the overall loss function, which is applied

for the trade-off between the time-sensitive and the time-independent representations of each event.

The whole optimization objective is the combination of the loss function in Eq. 12 and the predicate embedding regularization in Eqs. 5-9. Besides, our model is trained with the Adam optimizer (Kingma and Ba 2015) to learn the embeddings of entities, predicates, concepts and timestamps.

4 Experiments and Results

In this section, we introduce the experiment settings and exhibit some cases of temporal rules mined by our temporal rule learning algorithm. Then, the experimental results compared with some state-of-the-art baselines are provided to demonstrate the effectiveness of our model. Furthermore, the ablation study and case study are conducted.

4.1 Experiment Settings

Datasets. Three commonly used datasets of TKGs are used in the experiments, namely ICEWS14 (García-Durán, Dumančić, and Nieuport 2018), ICEWS05-15 (García-Durán, Dumančić, and Nieuport 2018) and Wikidata12k (Dasgupta, Ray, and Talukdar 2018). Both ICEWS14 and ICEWS05-15 contain political events with specific timestamps. Wikidata12k (Dasgupta, Ray, and Talukdar 2018) is a subset of Wikidata (Erxleben et al. 2014), in which each time annotation is a timestamp or time interval. For each dataset, all the events are split into training, validation and test sets in a proportion of 80%/10%/10% following some previous works (Lacroix, Obozinski, and Usunier 2020; Xu et al. 2020a). Statistics for these datasets are presented in Table 1.

Evaluation Protocol. On the consideration that the amount of entities in any TKG is much more than that of predicates, predicting entities is more challenging than predicting predicates. Thus, the temporal KG completion task usually focuses on entity prediction such as $(s, p, ?, t)$ where the ob-

Models		ICEWS14				ICEWS05-15				Wikidata12k			
		MRR	H@10	H@3	H@1	MRR	H@10	H@3	H@1	MRR	H@10	H@3	H@1
Typical Models	TransE	0.280	0.637	-	0.094	0.294	0.663	-	0.090	0.178	0.339	0.192	0.100
	DistMult	0.439	0.672	-	0.323	0.456	0.691	-	0.337	0.222	0.460	0.238	0.119
	ComplEx	0.467	0.716	0.527	0.347	0.481	0.729	0.535	0.362	0.233	0.436	0.253	0.123
	RotatE	0.418	0.690	0.478	0.291	0.304	0.595	0.355	0.164	0.221	0.461	0.236	0.116
	QuatE	0.471	0.712	0.530	0.353	0.482	0.727	0.529	0.370	0.230	0.416	0.243	0.125
TKGE Models	TTransE	0.255	0.601	-	0.047	0.271	0.616	-	0.085	0.172	0.329	0.185	0.096
	HyTE	0.297	0.655	0.416	0.108	0.316	0.681	0.445	0.116	0.253	0.483	0.197	0.147
	TeRo	0.562	0.732	0.621	0.468	0.586	0.795	0.668	0.469	0.299	0.507	0.329	0.198
	ATiSE	0.550	0.750	0.629	0.436	0.519	0.794	0.606	0.378	0.252	0.462	0.288	0.148
	TComplEx	0.610	0.770	0.660	0.530	0.660	0.800	0.710	0.590	0.331	0.539	0.357	0.233
	TeLM	0.625	0.774	0.673	0.545	0.678	0.823	0.728	0.599	0.332	0.542	0.360	0.231
Ours	LCGE	0.925	0.937	0.929	0.916	0.912	0.925	0.916	0.903	0.668	0.871	0.778	0.547
APG \uparrow (%)		30.0	16.3	25.6	37.1	23.4	10.2	18.8	30.4	33.6	32.9	41.8	31.6
RPG \uparrow (%)		48.0	21.1	38.0	68.1	34.5	12.4	25.8	50.7	101.2	60.7	119.3	136.8

Table 3: Temporal KG completion results on three datasets. H1, H3 and H10 represent Hits@1, Hits@3 and Hits@10, respectively. **Bold** values are the best results and the second-to-best results are underlined in all the models. APG and RPG indicate the absolute performance gains and the relative performance gains achieved by our model compared with the best-performing baseline TeLM. APG and RPG can be calculated by $APG = R_{ours} - R_{baseline}$ and $RPG = (R_{ours} - R_{baseline})/R_{baseline}$, where R_{ours} and $R_{baseline}$ denote the results of our model and the baseline TeLM, respectively.

ject is missing in this event. To achieve the prediction results, each entity e_i in the TKG namely the candidate entity is filled in the object position to reconstruct a candidate event quadruple (s, p, e_i, t) . Then, the score for evaluating the plausibility of each candidate event is obtained from the time-sensitive and time-independent representations according to Eq. 10 and Eq. 11, which is defined as

$$E_{pred}(e_i) = E_1(s, p, e_i, t) + \lambda \cdot E_2(s, p, e_i) \quad (15)$$

Baselines. We select two types of state-of-the-art baseline models for comparison:

(1) Some typical KGE models without time information, including TransE (Bordes et al. 2013), DistMult (Yang et al. 2015), ComplEx (Trouillon et al. 2016), RotatE (Sun et al. 2019) and QuatE (Zhang et al. 2019).

(2) The previous well-performed TKGE models, including TTransE (Leblay and Chekol 2018), HyTE (Dasgupta, Ray, and Talukdar 2018), ATiSE (Xu et al. 2020b), TeRo (Xu et al. 2020a), TComplEx (Lacroix, Obozinski, and Usunier 2020) and TeLM (Xu et al. 2021).

Metrics and Implementation Details. We rank all the candidate events according to their scores calculated by Eq. 15 in descending order. Then, the rank of the correct event of the i -th test instance is defined as $rank_i$. We employ two commonly-used metrics for evaluating the results of TKG:

(1) The reciprocal mean rank (MRR) of the correct events,

which can be calculated by

$$MRR = \frac{1}{N} \cdot \sum_i^N \frac{1}{rank_i} \quad (16)$$

where N is the total amount of test instances.

(2) The ratio of the correct events ranked in the top n (Hits@ n), which is calculated by

$$Hits@n = \frac{1}{N} \cdot \sum_i^N \mathbb{I}(rank_i \leq n) \quad (17)$$

where the value of function $\mathbb{I}(rank_i \leq n)$ is 1 if $rank_i \leq n$ is true. n is usually set as 1, 3 or 10. Note that the higher MRR and Hits@ n indicate better performance.

In particular, our model represents the timeliness of each event with its timestamp, it is necessary to convert an event with a time interval in wikidata12k into two events along with the timestamps at both ends of the time interval. In the inference stage, the score of each event with a time interval in wikidata12k is achieved by averaging the individual scores of two events with endpoint timestamps of the time interval. Besides, the open-source rule learning tool AMIE+ (Galárraga et al. 2015) is utilized to mine the static rules for its convenience and good performance.

We conduct all the experiments in Pytorch and on a GeForce GTX 2080Ti GPU. The batch size is set as 1024.

Models	ICEWS14				ICEWS05-15			
	MRR	Hits@10	Hits@3	Hits@1	MRR	Hits@10	Hits@3	Hits@1
LCGE	0.925	0.937	0.929	0.916	0.912	0.925	0.916	0.903
-RGPR	0.850	0.882	0.867	0.826	0.722	0.819	0.754	0.668
-TIS	0.693	0.816	0.741	0.623	0.586	0.795	0.668	0.469

Table 4: Ablation study of eliminating RGPR module and time-independent score from the whole model LCGE.

The thresholds of SC and HC in our temporal rule learning algorithm are both fixed to 0.1 on all the datasets. We tune the hyper-parameters by grid search on the validation sets. Specifically, the dimension of embeddings d is selected in the range of $\{100, 200, 500, 1000, 2000\}$. The dimension of embeddings specific to commonsense k is set as the half of d . The learning rate l_r is tuned in $\{0.01, 0.05, 0.1, 0.5\}$, the weights of N3 regularization α_1 and α_2 are chosen in $\{0.01, 0.1, 1.0, 2.0, 5.0\}$, the weight of commonsense in the whole loss function λ is adjusted in $\{0.5, 1.0, 2.0, 3.0, 5.0\}$.

4.2 Cases of Temporal Rules

Some cases of temporal rules mined by our temporal rule learning algorithm from ICEWS05-15 are exhibited in Table 2. We observe that each temporal rule has a confidence level, which corresponds to the weight of the rule-guided predicate embedding regularization derived from this rule. These temporal rules are friendly for humans to understand, which benefits the explainability of the predicted results.

4.3 Experimental Results

The comparison results between our LCGE model with both the traditional KGE models and the existing TKGE models are provided in Table 3. The results of all the baseline models on ICEWS14 and ICEWS05-15 are directly taken from the original paper of TeLM (Xu et al. 2021), and the experimental results of all baselines on Wikidata12k are obtained by running the source code corresponding to each baseline model. We observe that **our proposed LCGE model outperforms all the baselines consistently and significantly on all the datasets**. Particularly, compared with the best-performing baseline model TeLM, our approach obtains substantial performance improvements. The difference between TeLM and our model LCGE shown in Table 2 is statistically significant under the paired at the 99% significance level. In terms of the absolute performance gains (APG), our model achieves **30.0%/23.4%/33.6%** as to MRR and **37.1%/30.4%/31.6%** as to Hits@1 on ICEWS14/ICEWS05-15/Wikidata12k. With respect to the relative performance gains (RPG), our model achieves **48.0%/34.5%/101.2%** as to MRR and **68.1%/50.7%/136.8%** as to Hits@1 on ICEWS14/ICEWS05-15/Wikidata12k.

In particular, even though TeLM achieves merely 0.545 and 0.599 as to Hits@1 on ICEWS14 and ICEWS05-15, the performances of LCGE are both higher than 0.9 on these datasets. This result illustrates that our model guarantees satisfying accuracy on the challenging TKGC task. Besides, the recent TKGE baselines and our model LCGE all outperform the traditional KGE models, which emphasizes the

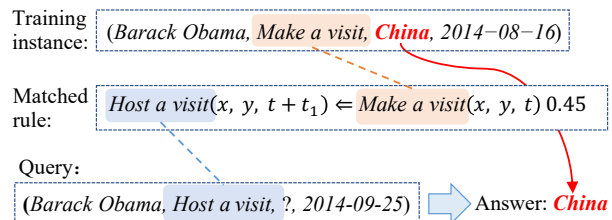


Figure 4: A case study of TKGC with explainability via the causality among events with a temporal rule.

significance of learning the time-sensitive representation of events for TKGC task. Furthermore, the more superior performance of our model compared with the TKGC baselines demonstrates the effectiveness of evaluating the plausibility of each event from the perspectives of both time-sensitive representation and time-independent commonsense.

4.4 Ablation Study

To verify the effectiveness of each module in our scheme, we observe the performances of two ablated models: (1) eliminating the RGPR module from the whole model (-RGPR), and (2) removing the time-independent score (-TIS) during both training and inference stages. The results of the ablation study as shown in Table 4 demonstrate that eliminating RGPR or TIS both has an obvious impact on the performance of the whole model. Besides, omitting TIS shows more performance drop, which suggests the vital role of predicting events in the view of commonsense. Furthermore, the number of high-quality temporal rules is limited, leading to relatively less performance improvement derived from temporal rules. The result on Wikidata12k is not presented since the number of high-quality temporal rules mined from Wikidata12k is too small to verify the effectiveness of the ablated model -RGPR. Thus, how to mine more temporal rules would be studied in-depth in future research.

4.5 Case Study

It is noteworthy that our approach could employ the symbolic temporal rules to declare the inference process explicitly and enhance the explainability that all the existing TKGE models are lack of. On account of a TKGC query (*China, Make a Visit, ?, 2012-11-16*) as shown in Figure 4, our model predicts the entity *South Korea* with the highest score. More particularly, a temporal rule *Host a visit(x, y, t + t₁) ⇔ Make a visit(x, y, t)* could be matched to the given query. Meanwhile, an event

(*China, Host a visit, South Korea, 2012-11-20*) in the training set shares the same subject with the query, which is a grounding of the head atom of the matched rule. Therefore, *South Korea* could be directly deduced by the temporal rule, which is consistent with the result obtained by our model and facilitates the explainability of the result.

5 Conclusion

In this paper, we propose a novel and effective logic and commonsense-guided embedding model LCGE for TKGC task. As far as we can be concerned, our model is the first to learn both the time-sensitive representation of events involving timeliness and causality as well as the time-independent commonsense representation, simultaneously. Specifically, the causality among events could be learned via our temporal rule learning algorithm and the temporal rule-guided predicate embedding regularization. The experimental results of the TKGC task on three datasets illustrate the significant performance improvements obtained by our model LCGE compared with the state-of-the-art baselines. More interestingly, our model could provide the explainability of results according to causality inference via temporal rules.

Acknowledgements

This work was partially supported by Zhejiang Science and Technology Plan Project (No. 2022C01082), the National Natural Science Foundation of China (No. 62072022, 61772054) and the Fundamental Research Funds for the Central Universities.

References

Bordes, A.; Usunier, N.; Garcia-Duran, A.; Weston, J.; and Yakhnenko, O. 2013. Translating embeddings for modeling multi-relational data. In *Proceedings of the 26th International Conference on Neural Information Processing Systems*, 2787–2795.

Cao, Z.; Xu, Q.; Yang, Z.; Cao, X.; and Huang, Q. 2021. Dual Quaternion Knowledge Graph Embeddings. In *Proceedings of the AAAI Conference on Artificial Intelligence*, 6894–6902.

Dasgupta, S. S.; Ray, S. N.; and Talukdar, P. 2018. HyTE: Hyperplane-based Temporally aware Knowledge Graph Embedding. In *Proceedings of the 2018 Conference on Empirical Methods in Natural Language Processing*, 2001–2011.

Erxleben, F.; Günther, M.; Krötzsch, M.; Mendez, J.; and Vrandečić, D. 2014. Introducing Wikidata to the Linked Data Web. In *Proceedings of the International Semantic Web Conference*, 50–65.

Galárraga, L.; Teffouli, C.; Hose, K.; and Suchanek, F. 2015. Fast rule mining in ontological knowledge bases with AMIE+. *The VLDB Journal*, 24(6): 707–730.

García-Durán, A.; Dumančić, S.; and Niepert, M. 2018. Learning Sequence Encoders for Temporal Knowledge Graph Completion. In *Proceedings of the 2018 Conference on Empirical Methods in Natural Language Processing*, 4816–4821.

Goel, R.; Kazemi, S. M.; Brubaker, M.; and Poupart, P. 2020. Diachronic Embedding for Temporal Knowledge Graph Completion. In *Proceedings of the AAAI Conference on Artificial Intelligence*, 3988–3995.

Ho, V. T.; Stepanova, D.; Gad-Elrab, M. H.; Kharlamov, E.; and Weikum, G. 2018. Rule Learning From Knowledge Graphs Guided by Embedding Models. In *International Semantic Web Conference*, 72–90.

Jin, W.; Qu, M.; Jin, X.; and Ren, X. 2020. Recurrent Event Network: Autoregressive Structure Inference over Temporal Knowledge Graphs. In *Proceedings of the 2020 Conference on Empirical Methods in Natural Language Processing*, 6669–6683.

Kingma, D. P.; and Ba, J. 2015. Adam: A method for stochastic optimization. In *Proceedings of the 3rd International Conference on Learning Representations*.

Lacroix, T.; Obozinski, G.; and Usunier, N. 2020. Tensor Decompositions for Temporal Knowledge Base Completion. In *Proceedings of the International Conference on Learning Representations*.

Leblay, J.; and Chekol, M. W. 2018. Deriving Validity Time in Knowledge Graph. In *Companion Proceedings of the The Web Conference 2018*, 1771–1776.

Meilicke, C.; Chekol, M. W.; Ruffinelli, D.; and Stuckschmidt, H. 2019. Anytime Bottom-Up Rule Learning for Knowledge Graph Completion. In *Proceedings of the 28th International Joint Conference on Artificial Intelligence*, 3137–3143.

Nickel, M.; Tresp, V.; and Kriegel, H.-P. 2011. A three-way model for collective learning on multi-relational data. In *Proceedings of the 28th International Conference on Machine Learning*, 809–816.

Omran, P. G.; Wang, K.; and Wang, Z. 2019a. An embedding-based approach to rule learning in knowledge graphs. In *IEEE Transactions on Knowledge and Data Engineering*, 1–12.

Omran, P. G.; Wang, K.; and Wang, Z. 2019b. Learning Temporal Rules from Knowledge Graph Streams. In *AAAI Spring Symposium: Combining Machine Learning with Knowledge Engineering*.

Qu, M.; Chen, J.; Xhonneux, L.-P.; Bengio, Y.; and Tang, J. 2021. RNNLogic: Learning Logic Rules for Reasoning on Knowledge Graphs. In *Proceedings of the 9th International Conference on Learning Representations*.

Sadeghian, A.; Armandpour, M.; Ding, P.; and Wang, D. Z. 2019. DRUM: End-To-End Differentiable Rule Mining On Knowledge Graphs. In *Proceedings of the 33rd International Conference on Neural Information Processing Systems*.

Speer, R.; Chin, J.; and Havasi, C. 2017. ConceptNet 5.5: An Open Multilingual Graph of General Knowledge. In *Proceedings of the Thirty-First AAAI Conference on Artificial Intelligence*, 4444–4451.

Sun, Z.; Deng, Z.-H.; Nie, J.-Y.; and Tang, J. 2019. RotatE: Knowledge Graph Embedding by Relational Rotation in Complex Space. In *Proceedings of the 7th International Conference on Learning Representations*.

Trivedi, R.; Dai, H.; Wang, Y.; and Song, L. 2017. Know-Evolve: Deep Temporal Reasoning for Dynamic Knowledge Graphs. In *Proceedings of the 34th International Conference on Machine Learning*, 3462–3471.

Trouillon, T.; Welbl, J.; Riedel, S.; Éric Gaussier; and Bouchard, G. 2016. Complex embeddings for simple link prediction. In *Proceedings of the 33rd International Conference on Machine Learning*, 2071–2080.

Wang, Z.; Zhang, J.; Feng, J.; and Chen, Z. 2014. Knowledge graph embedding by translating on hyperplanes. In *Proceedings of the AAAI Conference on Artificial Intelligence*, 1112–1119.

Xu, C.; Chen, Y.; Nayyeri, M.; and Lehmann, J. 2021. Temporal Knowledge Graph Completion Using a Linear Temporal Regularizer and Multivector Embeddings. In *Proceedings of the 2021 Conference of the North American Chapter of the Association for Computational Linguistics*, 2569–2578.

Xu, C.; Nayyeri, M.; Alkhouri, F.; Shariat Yazdi, H.; and Lehmann, J. 2020a. TeRo: A Time-aware Knowledge Graph Embedding via Temporal Rotation. In *Proceedings of the 28th International Conference on Computational Linguistics*, 1583–1593.

Xu, C.; Nayyeri, M.; Alkhouri, F.; Yazdi, H.; and Lehmann, J. 2020b. Temporal knowledge graph completion based on time series gaussian embedding. In *International Semantic Web Conference*, 654–671.

Yang, B.; tau Yih, W.; He, X.; Gao, J.; and Deng, L. 2015. Embedding entities and relations for learning and inference in knowledge bases. In *Proceedings of the 3rd International Conference on Learning Representations*.

Y.Chen; D.Z.Wang; and S.Goldberg. 2016. ScaLeKB: Scalable Learning and Inference Over Large Knowledge Bases. *VLDB Journal*, 25: 893–918.

Zhang, S.; Tay, Y.; Yao, L.; and Liu, Q. 2019. Quaternion Knowledge Graph Embeddings. In *Proceedings of the 33rd International Conference on Neural Information Processing Systems*, 2731–2741.

Zhu, C.; Chen, M.; Fan, C.; Cheng, G.; and Zhang, Y. 2021. Learning from History: Modeling Temporal Knowledge Graphs with Sequential Copy-Generation Networks. In *Proceedings of the 35th AAAI Conference on Artificial Intelligence*, 4732–4740.

A Appendix

A.1 Description of the Temporal Rule Patterns

(1) $p_2(x, y, t + t_1) \Leftarrow p_1(x, y, t)$. With regard to a length-1 rule, the body atom $p_1(x, y, t)$ and the head atom $p_2(x, y, t + t_1)$ occur at different times. This temporal rule pattern signifies that two events containing predicates p_1 and p_2 would occur one after the other if both the subject and object are the same, respectively. For instance, given a temporal rule $Consult(x, y, t + t_1) \Leftarrow Express\ intent\ to\ meet\ or\ negotiate(x, y, t)$ and an event $(China, Express\ intent$

$to\ meet\ or\ negotiate, U.S.A., TS_1)$ occurring at the timestamp TS_1 , we could easily deduce that an event $(China, Consult, U.S.A., TS_1 + T)$ will happen after TS_1 .

(2) $p_2(x, y, t) \Leftarrow p_1(x, y, t)$. For a length-1 rule, the body atom $p_1(x, y, t)$ and the head atom $p_2(x, y, t)$ occur simultaneously. This pattern is equivalent to the length-1 static rule.

(3) $p_3(x, y, t + t_1 + t_2) \Leftarrow p_1(x, z, t) \wedge p_2(z, y, t + t_1)$. The three atoms in this pattern of temporal rule occur at different time from each other. This pattern implies the three causally related events occur one after the other. For instance, the temporal rule $Express\ intent\ to\ meet\ or\ negotiate(x, y, t + t_1 + t_2) \Leftarrow Engage\ in\ negotiation^{-1}(x, z, t) \wedge Express\ intent\ to\ cooperate(z, y, t + t_1)$ belongs to this temporal rule pattern, where the predicate $Engage\ in\ negotiation^{-1}$ is the inverse version of the predicate $Engage\ in\ negotiation$.

(4) $p_3(x, y, t + t_1) \Leftarrow p_1(x, z, t) \wedge p_2(z, y, t)$. Specific to this rule pattern, the two events corresponding to the body atoms $p_1(x, z, t)$ and $p_2(z, y, t)$ such as (s, p_1, e, t) and (e, p_2, o, t) occur at the timestamp t , and then the event $(s, p_3, o, t + t_1)$ associated with the atom $p_3(x, y, t + t_1)$ would happen.

(5) $p_3(x, y, t) \Leftarrow p_1(x, z, t) \wedge p_2(z, y, t)$. Similar to the pattern (2), this pattern of the temporal rule indicates that all the events corresponding to the atoms occur at the same time, which is equivalent to the length-2 static rule.

A.2 Evaluation Criteria of Length-2 Temporal Rules

For the length-2 candidate temporal rule in the general form of $p_3(x, y, t + T_1 + T_2) \Leftarrow p_1(x, z, t) \wedge p_2(z, y, t + T_1)$, there are three diverse patterns with the different values of T_1 and T_2 . In allusion to each timestamp t , the SD, SC and HC are defined as:

$$SD =$$

$$\begin{cases} \sum_{t_{1i} \in [1, W_T]} \sum_{t_{2i} \in [1, W_T]} \#(a, c) : p_1(a, b, t) \\ \wedge p_2(b, c, t + t_{1i}) \wedge p_3(a, c, t + T_{1i} + T_{2i}), & T_1 > 0, T_2 > 0 \\ \sum_{t_{2i} \in [1, W_T]} \#(a, c) : p_1(a, b, t) \wedge p_2(b, c, t) \\ \wedge p_3(a, c, t + t_{2i}), & T_1 = 0, T_2 > 0 \\ \#(a, c) : p_1(a, b, t) \wedge p_2(b, c, t) \wedge p_3(a, c, t), & T_1 = T_2 = 0 \end{cases} \quad (18)$$

$$SC =$$

$$\begin{cases} \frac{1}{|W_T|} \cdot \frac{SD}{\sum_{t_{1i} \in [1, W_T]} \#(a, c) : p_1(a, b, t) \wedge p_2(b, c, t + t_{1i})}, & T_1 > 0 \\ \frac{SD}{\#(a, c) : p_1(a, b, t) \wedge p_2(b, c, t)}, & T_1 = 0 \end{cases} \quad (19)$$

$$\begin{cases} \frac{SD}{\sum_{t_{1i} \in [1, W_T]} \sum_{t_{2i} \in [1, W_T]} \#(a, c) : p_3(a, c, t + t_{1i} + t_{2i})}, & T_1 > 0, T_2 > 0 \\ \frac{SD}{\sum_{t_{1i} \in [1, W_T]} \#(a, c) : p_3(a, c, t + t_{1i} + t_{2i})}, & T_1 = 0, T_2 > 0 \\ \frac{SD}{\#(a, c) : p_3(a, c, t)}, & T_1 = T_2 = 0 \end{cases} \quad (20)$$

It is noteworthy that the temporal rule with the settings (1) $T_1 > 0, T_2 > 0$, (2) $T_1 > 0, T_2 = 0$, (3) $T_1 = T_2 = 0$ correspond to the temporal rule patterns (3), (4) and (5).

A.3 The Algorithm of Our Proposed Temporal Rule Learning Module

For better understanding, Algorithm 1 summarizes the whole procedure of our temporal rule learning procedure.

Algorithm 1: our temporal rule learning module.

```

1 Input:  $\mathcal{G}_s, \mathcal{G}_t$ : the GSKG and the TKG
    $T, W_T$ : the number of timestamps and the
   size of time window
    $T_{sc}, T_{hc}$ : the thresholds of SC and HC of
   temporal rules
2 Output:  $\mathcal{R}_t$ : the set of temporal rules satisfying  $T_{sc}$ 
   and  $T_{hc}$ 
3 Mine static rules by a rule mining tool such as
   AMIE+ from  $\mathcal{G}_s$ ;
4 Convert each static rule into candidate temporal
   rules via temporal rule patterns;
5 while select a candidate temporal rule  $Ru$  do
6   for  $t=1,2,\dots, T$  do
7     Generate two sub-graphs  $\mathcal{G}_{s1}$  and  $\mathcal{G}_{s2}$  via
       fusing the events in the time intervals  $[t+1,$ 
        $t+W_T]$  and  $[t+W_T+1, t+2W_T]$  from  $\mathcal{G}_t$ ;
8     if the length of  $Ru$  is 1 then
9       Calculate the SC and HC of  $Ru$  by
       Eqs. 2-4;
10    else
11      Calculate the SC and HC of  $Ru$  by
       Eqs. 18-20;
12    if the mean value of SC and HC at all the
       timestamps are both higher than  $T_{sc}$  and  $T_{hc}$ 
       then
13      Add  $Ru$  into  $\mathcal{R}_t$ ;

```

A.4 Proof of Representing Causality Among Events via RGPR Mechanism

In this paper, we take the temporal rule patterns (1) and (3) as examples, and provide the lemma proofs that the temporal rule-guided predicate embedding regularization \mathbf{G} could represent the causality among events.

Lemma 1. On account of the temporal rule pattern (1) $p_2(x, y, t+t_1) \Leftarrow p_1(x, y, t)$, the temporal rule-guided predicate embedding regularization \mathbf{G} specific to Eq. 5 could represent the causality between two events.

Proof. Given an event (s, p_1, o, t) , we could obtain the causality term of the time-sensitive score specific to this event transformed at the timestamp $t+t_1$ according to Eq. 10 and the time transfer operator \mathbf{T} , which can be written as

$$\text{Re}(\mathbf{s}^\top \text{diag}(\mathbf{T} \circ \mathbf{p}_{r1}) \bar{\mathbf{o}}) = 1 \quad (21)$$

According to \mathbf{G} defined in Eq. 5, the association between \mathbf{p}_{r1} and \mathbf{p}_{r2} satisfies:

$$\mathbf{T} \circ \mathbf{p}_{r1} = \mathbf{p}_{r2} \quad (22)$$

Substituting Eq. 22 into Eq. 21, we can derive that

$$\text{Re}(\mathbf{s}^\top \text{diag}(\mathbf{p}_{r2}) \bar{\mathbf{o}}) = 1 \quad (23)$$

It can be discovered that the event $(s, p_2, o, t+t_1)$ holds if (s, p_1, o, t) occurs. Therefore, the causality between two events occurring at different timestamps could be represented via the temporal rule-guided predicate embedding regularization \mathbf{G} of the pattern (1) defined in Eq. 5. \square

Lemma 2. For the temporal rule pattern $p_3(x, y, t+t_1 + t_2) \Leftarrow p_1(x, z, t) \wedge p_2(z, y, t+t_1)$, the temporal rule-guided predicate embedding regularization in Eq. 7 can represent the causality among three events at different timestamps.

Proof. If there are two events (s, p_1, e, t) and $(e, p_2, o, t+t_1)$ holds, the causality term of the time-sensitive scores specific to these two events transformed to the timestamp $t+t_1+t_2$ are achieved according to Eq. 10 as follows:

$$\text{Re}(\mathbf{s}^\top \text{diag}(\mathbf{T} \circ \mathbf{T} \circ \mathbf{p}_{r1}) \bar{\mathbf{e}}) = 1 \quad (24)$$

$$\text{Re}(\mathbf{e}^\top \text{diag}(\mathbf{T} \circ \mathbf{p}_{r2}) \bar{\mathbf{o}}) = 1 \quad (25)$$

In terms of the following equation

$$\begin{aligned} & \mathbf{s}^\top \text{diag}(\mathbf{T} \circ \mathbf{T} \circ \mathbf{p}_{r1}) \bar{\mathbf{e}} \mathbf{e}^\top \text{diag}(\mathbf{T} \circ \mathbf{p}_{r2}) \bar{\mathbf{o}} \\ &= \mathbf{s}^\top \text{diag}(\mathbf{T} \circ \mathbf{T} \circ \mathbf{p}_{r1} \circ \mathbf{T} \circ \mathbf{p}_{r2}) \bar{\mathbf{o}} \end{aligned} \quad (26)$$

and Eqs. 24 and 25, we could derive that

$$\text{Re}(\mathbf{s}^\top \text{diag}(\mathbf{T} \circ \mathbf{T} \circ \mathbf{p}_{r1} \circ \mathbf{T} \circ \mathbf{p}_{r2}) \bar{\mathbf{o}}) = 1 - \quad (27)$$

$$\text{Im}(\mathbf{s}^\top \text{diag}(\mathbf{T} \circ \mathbf{T} \circ \mathbf{p}_{r1}) \bar{\mathbf{e}}) \cdot \text{Im}(\mathbf{e}^\top \text{diag}(\mathbf{T} \circ \mathbf{p}_{r2}) \bar{\mathbf{o}})$$

Furthermore, if the following equation

$$\text{Im}(\mathbf{s}^\top \text{diag}(\mathbf{T} \circ \mathbf{T} \circ \mathbf{p}_{r1}) \bar{\mathbf{e}}) \cdot \text{Im}(\mathbf{e}^\top \text{diag}(\mathbf{T} \circ \mathbf{p}_{r2}) \bar{\mathbf{o}}) = 0 \quad (28)$$

is satisfied, Eq. 27 can be rewritten as:

$$\text{Re}(\mathbf{s}^\top \text{diag}(\mathbf{T} \circ \mathbf{T} \circ \mathbf{p}_{r1} \circ \mathbf{T} \circ \mathbf{p}_{r2}) \bar{\mathbf{o}}) = 1 \quad (29)$$

Substituting \mathbf{G} defined in Eq. 7 into Eq. 29, we can achieve

$$\text{Re}(\mathbf{s}^\top \text{diag}(\mathbf{p}_{r3}) \bar{\mathbf{o}}) = 1 \quad (30)$$

Therefore, we prove that the event $(s, p_3, o, t+t_1+t_2)$ is valid if (s, p_1, e, t) and $(e, p_2, o, t+t_1)$ successively occur via the temporal rule-guided predicate embedding regularization \mathbf{G} of the pattern (3), which indicates the causality among three events occurring at different timestamps. \square

The proofs of the causality among events corresponding to the other three temporal rule patterns modeled by our designed temporal rule-guided predicate embedding regularization \mathbf{G} can be obtained similarly to the above proofs.

From the proofs corresponding to Lemma 1 and Lemma 2, the causality term in the time-sensitive score of a candidate event causally related to the other already occurred events would be a higher value. More interestingly, it can explain the effectiveness of representing the causality of events via our temporal rule-guided predicate embedding regularization mechanism and facilitate higher accuracy of TKGC.